

# Non-chondritic sulphur isotope composition of the terrestrial mantle

J. Labidi<sup>1</sup>, P. Cartigny<sup>1</sup> & M. Moreira<sup>2</sup>

**Core-mantle differentiation is the largest event experienced by a growing planet during its early history. Terrestrial core segregation imprinted the residual mantle composition by scavenging siderophile (iron-loving) elements such as tungsten, cobalt and sulphur. Cosmochemical constraints suggest that about 97% of Earth's sulphur should at present reside in the core<sup>1</sup>, which implies that the residual silicate mantle should exhibit fractionated  $^{34}\text{S}/^{32}\text{S}$  ratios according to the relevant metal-silicate partition coefficients<sup>2</sup>, together with fractionated siderophile element abundances. However, Earth's mantle has long been thought to be both homogeneous and chondritic for  $^{34}\text{S}/^{32}\text{S}$ , similar to Canyon Diablo troilite<sup>3-6</sup>, as it is for most siderophile elements. This belief was consistent with a mantle sulphur budget dominated by late-accreted chondritic components. Here we show that the mantle, as sampled by mid-ocean ridge basalts from the south Atlantic ridge, displays heterogeneous  $^{34}\text{S}/^{32}\text{S}$  ratios, directly correlated to the strontium and neodymium isotope ratios  $^{87}\text{Sr}/^{86}\text{Sr}$  and  $^{143}\text{Nd}/^{144}\text{Nd}$ . These isotope trends are compatible with binary mixing between a low- $^{34}\text{S}/^{32}\text{S}$  ambient mantle and a high- $^{34}\text{S}/^{32}\text{S}$  recycled component that we infer to be subducted sediments. The depleted end-member is characterized by a significantly negative  $\delta^{34}\text{S}$  of  $-1.28 \pm 0.33\%$  that cannot reach a chondritic value even when surface sulphur (from continents, altered oceanic crust, sediments and oceans) is added. Such a non-chondritic  $^{34}\text{S}/^{32}\text{S}$  ratio for the silicate Earth could be accounted for by a core-mantle differentiation record in which the core has a  $^{34}\text{S}/^{32}\text{S}$  ratio slightly higher than that of chondrites ( $\delta^{34}\text{S} = +0.07\%$ ). Despite evidence for late-veener addition of siderophile elements (and therefore sulphur) after core formation, our results imply that the mantle sulphur budget retains fingerprints of core-mantle differentiation.**

Earlier reports of mid-ocean ridge basalts (MORBs)  $\delta^{34}\text{S}$  (where  $\delta^{34}\text{S} = [(^{34}\text{S}/^{32}\text{S})_{\text{sample}} / (^{34}\text{S}/^{32}\text{S})_{\text{CDT}} - 1] \times 1,000$  and CDT is Canyon Diablo troilite) yielded values statistically indistinguishable from the reported chondrite average of  $0.04 \pm 0.31\%$  (refs 3–6), consistent with a late-veener origin for sulphur in the mantle. This view has been recently questioned in a study using improved sulphur-extraction techniques<sup>7</sup>. Worldwide MORBs exhibit exclusively negative  $\delta^{34}\text{S}$  ranging down to  $-1.9\%$ , with an approximately 2‰ variability<sup>7</sup>. These observations raise questions as to whether the terrestrial mantle is chondritic in sulphur isotopes, but the mechanisms controlling MORB  $^{34}\text{S}/^{32}\text{S}$  variability remain unclear.

To address these issues, we investigated the sulphur isotope composition of 23 glasses dredged on the South Atlantic ridge between  $40^\circ$  and  $55^\circ$  S. Previous radiogenic isotopes<sup>8–10</sup>, noble gases<sup>11,12</sup>, volatiles<sup>13</sup>, major-element<sup>14</sup> and trace-element<sup>15</sup> measurements on these basalts illustrate interactions of the Shona–Discovery hotspots with the ridge. Several of the typical mantle end-members feed the mantle source of the two plumes, including HIMU ('high- $\mu$ ' where  $\mu = ^{238}\text{U}/^{204}\text{Pb}$ ), LOMU ('low- $\mu$ '), and enriched-mantle components. The samples analysed were chosen to reflect this geochemical variability and thus offer an opportunity to address  $^{34}\text{S}/^{32}\text{S}$  variations with respect to these mantle heterogeneities.

In our samples, sulphur occurs only in its reduced form, as commonly found in MORBs<sup>16–18</sup>, and the sulphur content, from 642 to 1,388 parts per million (p.p.m.), correlates with the FeO content (Supplementary Fig. 3A), illustrating magmatic sulphide saturation<sup>16</sup>. The eruption depth of our samples precludes any significant sulphur degassing<sup>19</sup>, restricting the sulphur isotope discussion to primary magmatic considerations.  $\delta^{34}\text{S}$  varies between  $-1.80\%$  and  $+1.05\%$ , whereas both the quantifying mass-independent signatures  $\Delta^{33}\text{S}$  and  $\Delta^{36}\text{S}$  (where  $\Delta^{33}\text{S} = \delta^{33}\text{S} - 1,000 \times [(\delta^{34}\text{S}/1,000 + 1)^{0.515} - 1]$  and  $\Delta^{36}\text{S} = \delta^{36}\text{S} - 1,000 \times [(\delta^{34}\text{S}/1,000 + 1)^{1.889} - 1]$ ), are homogeneous and equal within uncertainty to those of Canyon Diablo troilite (Supplementary Table 1). Besides,  $\delta^{34}\text{C}$  is remarkably correlated to source enrichment proxies such as  $^{87}\text{Sr}/^{86}\text{Sr}$  or  $^{143}\text{Nd}/^{144}\text{Nd}$  (Fig. 1). Seawater sulphate ( $\delta^{34}\text{S} = +21\%$ ) assimilation by erupted basalts could result in an increase in  $\delta^{34}\text{S}$ ; it would, however, scatter or erase any correlations between  $\delta^{34}\text{S}$  and tracers that remain insensitive to seawater incorporation (such as  $^{143}\text{Nd}/^{144}\text{Nd}$ ). It would also result in a relationship between  $\delta^{34}\text{S}$  and proxies of seawater incorporation such as chlorine contents or Cl/K ratios, which is again not the case (Supplementary Fig. 4). Correlated  $\delta^{34}\text{S}$  and radiogenic isotope enrichments thus reflect the variability of the MORB sources.

All the samples are saturated with immiscible sulphide<sup>16</sup>, and the extremely low osmium contents in the most primitive MORBs probably indicates that they were already sulphide-saturated during melting<sup>10</sup>. Such a saturation mechanism prevents us from constraining the sulphur contents of the mantle source, and because the fractionation factor between dissolved sulphur and magmatic sulphide might be significant, it raises the question of whether basalts can preserve the  $^{34}\text{S}/^{32}\text{S}$  ratios of their mantle source. Those basalts investigated have such distinct differentiation and melting histories<sup>14,15</sup> that the amount of sulphide left during both melting and differentiation is variable<sup>10,16</sup>. If the high-temperature sulphur isotope fractionation during magmatic sulphide exsolution were significant, it would have erased the observed  $\delta^{34}\text{S}$ – $^{87}\text{Sr}/^{86}\text{Sr}$ – $^{143}\text{Nd}/^{144}\text{Nd}$  trends (Fig. 1). The lack of correlation between  $\delta^{34}\text{S}$  and sulphide segregation proxies indicates a fractionation factor,  $\alpha_{\text{sulph-melt}}$ , of between 1.0000 and  $0.9995 \pm 0.0005$ , at most (Supplementary Information). The  $\delta^{34}\text{S}$  of basalts hence provides direct information on mantle source composition, here displaying an average value of  $-0.80 \pm 0.58\%$  ( $1\sigma$ ).

The most  $^{34}\text{S}$ -depleted samples correspond to depleted MORB and  $^{34}\text{S}$ -enriched samples are related to the Discovery plume, whereas the Shona and LOMU basalts are of intermediate composition. Interestingly, samples from Shona and Discovery display similar  $^3\text{He}/^4\text{He}$  and  $^{21}\text{Ne}/^{22}\text{Ne}$  (refs 11 and 12) but have different  $^{34}\text{S}$  enrichments, suggesting that these isotopic systems are decoupled. Such a lack of correlation between noble gases and S isotopes suggests that the primitive mantle is sulphur-poor compared to the recycled components. Hence, characterization of the primordial sulphur cannot be directly achieved from the present data set.

Our results can be explored in two ways. First, the south Atlantic depleted mantle has an average  $\delta^{34}\text{S}$  of  $-1.28 \pm 0.33\%$  (error is  $1\sigma$ ,

<sup>1</sup>Laboratoire de Géochimie des Isotopes Stables, Institut de Physique du Globe de Paris, Sorbonne Paris Cité, Université Paris Diderot, UMR 7154 CNRS, 1 rue Jussieu, 75005 Paris, France. <sup>2</sup>Laboratoire de Géochimie et Cosmochimie, Institut de Physique du Globe de Paris, Sorbonne Paris Cité, Université Paris Diderot, UMR 7154 CNRS 1 rue Jussieu, 75005 Paris, France.

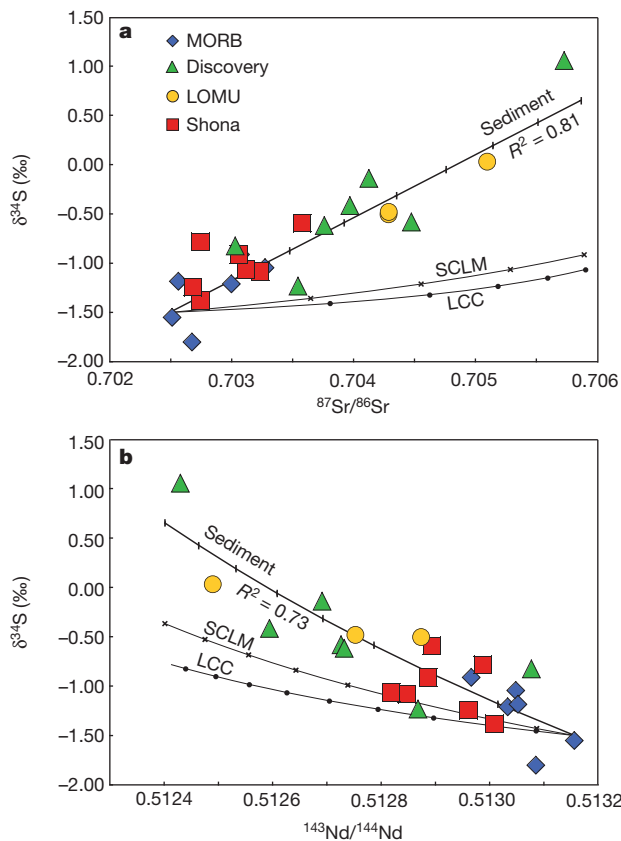


**Figure 1** |  $\delta^{34}\text{S}$  versus  $^{87}\text{Sr}/^{86}\text{Sr}$  and  $^{143}\text{Nd}/^{144}\text{Nd}$ . Strontium and neodymium isotope data are from ref. 8. Sulphur-isotope uncertainties are estimated on the basis of replicate analysis for all samples, and are all within symbol sizes. The samples define a binary mixing relationship between a depleted-mantle and an enriched-mantle endmember. Mixing trends with sub-continental lithospheric mantle (SCLM) and lower continental crust (LCC) are also shown, illustrating that mixing with sediments account better for the geochemical composition of our samples. **a**,  $\delta^{34}\text{S}$  versus  $^{87}\text{Sr}/^{86}\text{Sr}$ . **b**,  $\delta^{34}\text{S}$  versus  $^{143}\text{Nd}/^{144}\text{Nd}$ .  $\delta^{34}\text{S}$  is defined in the main text; the CDT standard is used.  $R$ , correlation coefficient. Data used for the mixing calculation is as follows, from refs 22–27 and Supplementary ref. 37. For depleted mantle,  $\delta^{34}\text{S} = -1.5\text{‰}$ ,  $^{87}\text{Sr}/^{86}\text{Sr} = 0.7025$ ,  $^{143}\text{Nd}/^{144}\text{Nd} = 0.513156$ ,  $\text{Sr} = 11.3$  p.p.m.,  $\text{Nd} = 1.12$  p.p.m. and  $\text{S} = 200$  p.p.m. For LCC,  $\delta^{34}\text{S} = +3\text{‰}$ ,  $^{87}\text{Sr}/^{86}\text{Sr} = 0.7080$ ,  $^{143}\text{Nd}/^{144}\text{Nd} = 0.511600$ ,  $\text{Sr} = 348$  p.p.m.,  $\text{Nd} = 11$  p.p.m. and  $\text{S} = 408$  p.p.m. For SCLM,  $\delta^{34}\text{S} = +3\text{‰}$ ,  $^{87}\text{Sr}/^{86}\text{Sr} = 0.7100$ ,  $^{143}\text{Nd}/^{144}\text{Nd} = 0.511663$ ,  $\text{Sr} = 49$  p.p.m.,  $\text{Nd} = 2.67$  p.p.m. and  $\text{S} = 157$  p.p.m. For the sediment,  $\delta^{34}\text{S} = +10\text{‰}$ ,  $^{87}\text{Sr}/^{86}\text{Sr} = 0.7203$ ,  $^{143}\text{Nd}/^{144}\text{Nd} = 0.511170$ ,  $\text{Sr} = 327$  p.p.m.,  $\text{Nd} = 27$  p.p.m. and  $\text{S} = 5,700$  p.p.m. Markers on the fits are separated by 0.1%, 1.0% and 4.0% for sediment, LCC and SCLM, respectively.

$n = 6$ ), defining a mean value consistently distinct from chondrites. We note that an extrapolation of Sr–Nd–S isotope trends to most depleted compositions would lead to a depleted-mantle endmember as low as  $-1.80\text{‰}$  (Fig. 1). Second, the nature of classical mantle endmembers can be addressed. Whereas it is commonly accepted that HIMU features reflect the occurrence of subducted oceanic crust in plume sources<sup>20</sup>, the enriched-mantle and LOMU cases remain much debated. In the south Atlantic mantle, a significant contribution of continental material has been invoked to account for the LOMU endmember, including either delaminated subcontinental lithospheric mantle<sup>8,9</sup> or lower continental crust<sup>10</sup>. In S–Sr and S–Nd isotope spaces, however, the samples lie on a linear trend regardless of their locations or type of anomalies (Fig. 1), highlighting binary mixing between depleted mantle ( $\delta^{34}\text{S} = -1.28\text{‰}$  or lower) and the enriched-mantle-type endmember ( $\delta^{34}\text{S} = +1.05\text{‰}$  or higher).

Both LOMU basalts (having the lowest  $^{206}\text{Pb}/^{204}\text{Pb}$ ) and Shona samples (HIMU-type<sup>8</sup>, having the highest  $^{206}\text{Pb}/^{204}\text{Pb}$ ) cannot be distinguished from the other samples in the observed trends (Fig. 1). This

lack of correlation between  $\delta^{34}\text{S}$  and  $^{206}\text{Pb}/^{204}\text{Pb}$  (Supplementary Fig. 5), together with the preservation of the trends between  $\delta^{34}\text{S}$  and Sr–Nd isotopes, argue in favour of relatively sulphur-poor HIMU and LOMU endmembers, overprinted by the contribution of a sulphur-rich enriched-mantle component. In this view, recycled oceanic crust carrying the radiogenic  $^{206}\text{Pb}/^{204}\text{Pb}$  ratio is inferred to be relatively sulphur-depleted, consistent with its required high U/Pb. Sulphides are indeed the main Pb carrier in the oceanic crust<sup>21</sup> and any Pb loss along subduction should occur through a concomitant sulphur loss.

The mixing trends being linear, the enriched-mantle component must be enriched in sulphur in the same way as it is enriched in strontium and neodymium. This allows a reliable estimate of its S/Sr and S/Nd, broadly equal to that of the depleted mantle. For simplicity, only the S/Sr ratio is used in the following. Taking  $200 \pm 40$  p.p.m. (ref. 22) for sulphur and 11.3 p.p.m. (ref. 15) for strontium in depleted mantle, we obtain an S/Sr value for enriched mantle of  $17 \pm 4$ . Both delaminated lithospheric mantle and lower continental crust have been suggested to account for enriched-mantle-type signals, especially in south Atlantic basalts<sup>8–10</sup>. These reservoirs are, however, relatively sulphur-poor compared to incompatible trace elements, yielding S/Sr ratios of  $3.2 \pm 2.0$  (ref. 23) and  $0.8 \pm 0.3$  (ref. 24), respectively, that are low compared to the required value of  $17 \pm 4$  (see above). Any occurrence of such a component in the south Atlantic mantle would have led to highly curved mixing relationships in S–Sr isotope space, especially given the range of  $^{87}\text{Sr}/^{86}\text{Sr}$  displayed by the samples (Fig. 1a).

Alternatively, sediment may be a good candidate: sediments are enriched in trace elements<sup>25</sup> and can bear significant amounts of sulphur. In particular, many sediments deposited one to two billion years ago during the Proterozoic eon formed under reduced conditions and usually contain more than 1% of sulphur pyrite<sup>26</sup>. A subducted sediment containing a realistic sulphur content of  $5,700 \pm 1,000$  p.p.m. would satisfy the S/Sr of the enriched-mantle component. The fact that our estimate for recycled sediment falls within large uncertainties of non-subducted sediments suggests only moderate devolatilization, if any, during recycling (Supplementary Information). The best fits to our data are obtained for sediment having a  $\delta^{34}\text{S}$  of  $+10 \pm 3\text{‰}$ , consistent with sediments one to two billion years old with an average  $\delta^{34}\text{S}$  of  $+5 \pm 10\text{‰}$  (ref. 27). This Proterozoic age for subducted sediments is also consistent with the observed lack of  $\Delta^{33}\text{S}$  variability<sup>28</sup> best-fitted with a  $\Delta^{33}\text{S}$  of  $+0.06 \pm 0.03\text{‰}$  (Supplementary Fig. 6).

If subducted sediments are major  $^{34}\text{S}$  carriers to the deep mantle, the depleted mantle is shown here to be significantly  $^{34}\text{S}$ -depleted with respect to chondrites. This low  $^{34}\text{S}/^{32}\text{S}$  ratio has fundamental implications for our understanding of the origin and processes affecting moderately volatile elements in the terrestrial mantle. In the following, we use the  $-1.28 \pm 0.33\text{‰}$  depleted MORB average as the representative  $\delta^{34}\text{S}$  of the depleted mantle, but further studies are needed to refine this value. Such a negative estimate allows us to discard a purely late-vener origin for sulphur in the mantle, because this scenario requires a strictly chondritic  $^{34}\text{S}/^{32}\text{S}$  ratio for depleted mantle. According to the kinetic theory of gases, partial evaporation of sulphur during accretion could have modified the  $^{34}\text{S}/^{32}\text{S}$  ratio of the accreted Earth, leaving the residual terrestrial mantle enriched in  $^{34}\text{S}$  relative to chondrites. This would be at odds with the observed depletion in  $^{34}\text{S}$ . Finally, assuming that the depleted mantle represents 25%–80% of the whole mantle<sup>29</sup>, the complementary surface reservoirs (continents, oceans and altered oceanic crust) would need to have an average  $\delta^{34}\text{S}$  of between  $+8\text{‰}$  and  $+25\text{‰}$  to balance the non-chondritic  $\delta^{34}\text{S}$  of the depleted mantle. Current estimates, however, yield average  $\delta^{34}\text{S}$  values of  $-0.4 \pm 3.0\text{‰}$  (ref. 30) for the bulk surface reservoirs, a value that is far from being reconcilable with the above requirement, and emphasizing the non-chondritic character of the bulk silicate Earth.

In contrast to immiscible sulphide exsolution, sulphur dissolution into metal from silicate could fractionate the  $^{34}\text{S}/^{32}\text{S}$  ratio owing to the distinct molecular environment of sulphur in a silicate versus a metallic liquid (and distinct vibrational partition functions). One likely possibility

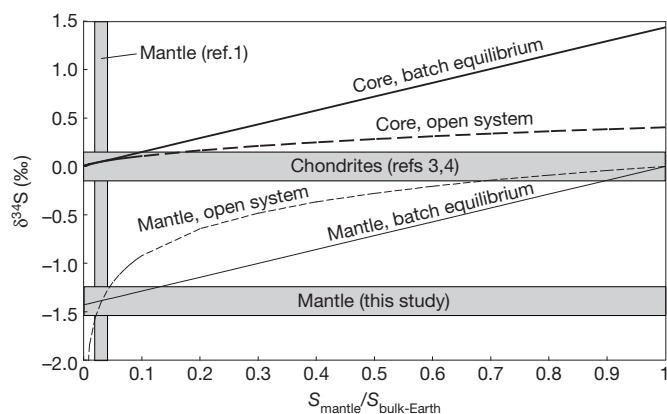


**Figure 2 | Core–mantle sulphur partitioning model in batch equilibrium or open system.** The  $\delta^{34}\text{S}$  of the mantle is plotted against the sulphur content of the mantle  $S_{\text{mantle}}$  divided by the sulphur content of the bulk Earth  $S_{\text{bulk-Earth}}$ . According to ref. 1,  $S_{\text{mantle}}$  represents less than 3% of  $S_{\text{bulk-Earth}}$ . The sulphur isotope composition of chondrites (refs 3 and 4) and mantle (this study) values are both plotted, allowing a clear visualization of the sulphur isotope shift between these two reservoirs. Sulphur isotope and sulphur abundance observations coincide at an anchor point constraining the core–mantle fractionation. Under batch equilibrium, core  $\delta^{34}\text{S}$  is +1.26‰ higher than the silicate value ( $\alpha_{\text{core-mantle}} = 1.00130$ ). In an open system model, the core is treated as a cumulative product and  $\alpha_{\text{core-mantle}}$  of 1.00035 is sufficient to explain the shift between mantle and chondrites.

involves the dissolution of sulphur in its metallic form ( $\text{S}^0$ ) in the core, given that stable isotope fractionation theory predicts the more oxidized compound to be  $^{34}\text{S}$ -enriched compared to sulphur dissolved as  $\text{S}^{2-}$  in the silicate mantle. The  $\alpha_{\text{core-mantle}}$  can be inferred from a chondritic bulk Earth (that is, mantle and core) by combining the distribution of sulphur in the bulk Earth (ref. 1) and the re-evaluated  $^{34}\text{S}/^{32}\text{S}$  of the mantle (this study), leading to a  $\alpha_{\text{core-mantle}}$  of 1.00130 for a batch-equilibrium or 1.00035 for an open-system sulphur incorporation into the core (Fig. 2). In all cases, the core  $\delta^{34}\text{S}$  is expected to be +0.07‰, almost indistinguishable from that of chondrites and iron meteorites, because this reservoir would contain most of the terrestrial sulphur<sup>1</sup>.

Only Shahar *et al.*<sup>2</sup> experimentally addressed the  $^{34}\text{S}/^{32}\text{S}$  fractionation between metal and silicate at high temperature, and estimated a  $\alpha_{\text{core-mantle}}$  of  $1.00220 \pm 0.0014\%$  at 1,850 °C (ref. 2). For 97% of the sulphur occurring in the core<sup>1</sup>, such an estimate should lead to a mantle  $\delta^{34}\text{S}$  of  $-2.10 \pm 1.40\%$ , under batch-equilibrium fractionation. This value, despite a significant overlap, seems slightly lower than our observation. Because stable isotope fractionations scale with temperature  $T$  as  $1/T^2$ , such distinct estimates could reflect a core segregation occurring at a temperature higher than 1,850 °C: the average temperature for core–mantle segregation remains highly debated, with values up to 3,300 °C (ref. 31). Alternatively, such a distinction may require the involvement of ‘hybrid models’, as suggested for highly siderophile elements<sup>31</sup>, in which a fraction of the mantle sulphur is a fractionated leftover from core–mantle equilibrium, whereas the other fraction would have been delivered during the late-accretionary stage. For a  $\alpha_{\text{core-mantle}}$  of 1.00220 (ref. 2), the proportion of late-accreted sulphur (that is, with chondritic  $^{34}\text{S}/^{32}\text{S}$ ) in the mantle would reach approximately 40% of mantle sulphur, after batch-equilibrium core segregation.

At that stage, the most obvious implication of such a core–mantle differentiation record is that sulphur and elements of comparable volatilities (such as zinc, fluorine and lead) must have been present to some extent before the late-accretion event. This is a robust and independent constraint that will help to build more consistent models of timing for the origin of moderately volatile elements in Earth’s mantle.

## METHODS SUMMARY

Samples were analysed following the protocol described in ref. 7. Glassy rims of basalts were handpicked under a binocular microscope and if needed, cleaned

through a sonication in 99.9% ethanol. For each sample, about 300 mg was crushed to a fine powder (<100  $\mu\text{m}$ ) and dissolved in a 29 N HF + 2.1 M  $\text{CrCl}_2$  solution. Under these conditions, sulphur is released as  $\text{H}_2\text{S}$  and subsequently trapped as precipitated  $\text{Ag}_2\text{S}$ . Sulphur extraction yields are  $101 \pm 4\%$  for the 23 samples analysed in this study.

Weighed aliquots of silver sulphide were wrapped in aluminium foil and placed in Ni-reaction bombs for fluorination with purified  $\text{F}_2$  at 250 °C overnight. The  $\text{SF}_6$  produced was then purified using both cryogenic separation and gas chromatography. The purified  $\text{SF}_6$  was then quantified and analysed using a dual-inlet ThermoFinnigan MAT 253 mass spectrometer where  $m/z = 127^+$ ,  $128^+$ ,  $129^+$  and  $131^+$  ion beams are monitored. All the samples were replicated, yielding a  $\pm 0.1$ ,  $\pm 0.005$  and  $\pm 0.1\%$  uncertainty for  $\delta^{34}\text{S}$ ,  $\Delta^{33}\text{S}$  and  $\Delta^{36}\text{S}$ , respectively, consistent with the basalt internal standards processed in ref. 7.

**Online Content** Any additional Methods, Extended Data display items and Source Data are available in the online version of the paper; references unique to these sections appear only in the online paper.

Received 25 April; accepted 18 July 2013.

Published online 4 September 2013.

- Dreibus, G. & Palme, H. Cosmochemical constraints on the sulfur content in the Earth’s core. *Geochim. Cosmochim. Acta* **60**, 1125–1130 (1996).
- Shahar, A., Fei, Y., Liu, M. C. & Wang, J. Sulfur isotopic fractionation during the differentiation of Mars. *Geochim. Cosmochim. Acta* **73** (Suppl.), A1201 (2009).
- Gao, X. & Thiemens, M. Isotopic composition and concentration of sulfur in carbonaceous chondrites. *Geochim. Cosmochim. Acta* **57**, 3159–3169 (1993).
- Gao, X. & Thiemens, M. Variations of the isotopic composition of sulfur in enstatite and ordinary chondrites. *Geochim. Cosmochim. Acta* **57**, 3171–3176 (1993).
- Sakai, H., Marais, D. J., Ueda, A. & Moore, J. G. Concentrations and isotope ratios of carbon, nitrogen and sulfur in ocean-floor basalts. *Geochim. Cosmochim. Acta* **48**, 2433–2441 (1984).
- Chaussidon, M., Sheppard, S. M. F. & Michard, A. Hydrogen, sulphur and neodymium isotope variations in the mantle beneath the EPR at 12°50'N. *J. Geochem. Soc.* **3**, 325–337 (1991).
- Labidi, J., Cartigny, P., Birck, J. L., Assayag, N. & Bourrand, J. J. Determination of multiple sulfur isotopes in glasses: a reappraisal of the MORB  $\delta^{34}\text{S}$ . *Chem. Geol.* **334**, 189–198 (2012).
- Douglass, J., Schilling, J. G. & Fontignie, D. Plume-ridge interactions of the Discovery and Shona mantle plumes with the southern Mid-Atlantic Ridge (40°–55°S). *J. Geophys. Res.* **104**, 2941–2962 (1999).
- Andres, M., Blichert-Toft, J. & Schilling, J. G. Hafnium isotopes in basalts from the southern Mid-Atlantic Ridge from 40°S to 55°S: discovery and Shona plume-ridge interactions and the role of recycled sediments. *Geochem. Geophys. Geosyst.* **3**, 1–25 (2002).
- Escrig, S., Schiano, P., Schilling, J. G. & Allègre, C. Rhenium-osmium isotope systematics in MORB from the Southern Mid-Atlantic Ridge (40°–50°S). *Earth Planet. Sci. Lett.* **235**, 528–548 (2005).
- Moreira, M., Staudacher, T., Sarda, P., Schilling, J. G. & Allègre, C. J. A primitive plume neon component in MORB: the Shona ridge-anomaly, South Atlantic (51–52°S). *Earth Planet. Sci. Lett.* **133**, 367–377 (1995).
- Sarda, P., Moreira, M., Staudacher, T., Schilling, J. G. & Allègre, C. J. Rare gas systematics on the southernmost Mid-Atlantic Ridge: constraints on the lower mantle and the Dupal source. *J. Geophys. Res.* **105**, 5973–5996 (2000).
- Dixon, J. E., Leist, L., Langmuir, C. & Schilling, J. G. Recycled dehydrated lithosphere observed in plume influenced mid-ocean-ridge basalt. *Nature* **420**, 385–389 (2002).
- le Roux, P. J., le Roex, A. P. & Schilling, J. G. MORB melting processes beneath the southern Mid-Atlantic Ridge (40–55°S): a role for mantle plume-derived pyroxenite. *Contrib. Mineral. Petrol.* **144**, 206–229 (2002).
- le Roux, P. J. *et al.* Mantle heterogeneity beneath the southern Mid-Atlantic Ridge: trace element evidence for contamination of ambient asthenospheric mantle. *Earth Planet. Sci. Lett.* **203**, 479–498 (2002).
- Mathez, E. A. Sulfur solubility and magmatic sulfides in submarine basalt glass. *J. Geophys. Res.* **81**, 4269–4276 (1976).
- Wallace, P. & Carmichael, I. S. E. Sulfur in basaltic magmas. *Geochim. Cosmochim. Acta* **56**, 1863–1874 (1992).
- Métrich, N., Berry, A. J., O’Neill, H. S. C. & Susini, J. The oxidation state of sulfur in synthetic and natural glasses determined by X-ray absorption spectroscopy. *Geochim. Cosmochim. Acta* **73**, 2382–2399 (2009).
- Dixon, J. E., Clague, D. A. & Stolper, E. M. Degassing history of water, sulfur, and carbon in submarine lavas from Kilauea Volcano, Hawaii. *J. Geol.* **99**, 371–394 (1991).
- Cabral, R. A. *et al.* Anomalous sulphur isotopes in plume lavas reveal deep mantle storage of Archaean crust. *Nature* **496**, 490–493 (2013).
- Kelley, K., Plank, T., Ludden, J. & Staudigel, H. Composition of altered oceanic crust at ODP Sites 801 and 1149. *Geochem. Geophys. Geosyst.* **4**, 8910 (2003).
- O’Neill, H. S. C. The origin of the Moon and the early history of the Earth—a chemical model. Part 2: The Earth. *Geochim. Cosmochim. Acta* **55**, 1159–1172 (1991).
- McDonough, W. F. Constraints on the composition of the continental lithospheric mantle. *Earth Planet. Sci. Lett.* **101**, 1–18 (1990).
- Rudnick, R. L. & Gao, S. Composition of the continental crust. *Treat. Geochem.* **3**, 1–64 (2003).

25. Plank, T. & Langmuir, C. H. The chemical composition of subducting sediment and its consequences for the crust and mantle. *Chem. Geol.* **145**, 325–394 (1998).
26. Poulton, S. W., Fralick, P. W. & Canfield, D. E. The transition to a sulphidic ocean 1.84 billion years ago. *Nature* **431**, 173–177 (2004).
27. Canfield, D. E. & Farquhar, J. Animal evolution, bioturbation, and the sulfate concentration of the oceans. *Proc. Natl Acad. Sci. USA* **106**, 8123–8127 (2009).
28. Farquhar, J., Bao, H. & Thiemens, M. Atmospheric influence of Earth's earliest sulfur cycle. *Science* **289**, 756–758 (2000).
29. Caro, G. & Bourdon, B. Non-chondritic Sm/Nd ratio in the terrestrial planets: consequences for the geochemical evolution of the mantle–crust system. *Geochim. Cosmochim. Acta* **74**, 3333–3349 (2010).
30. Wedepohl, K. H. The composition of the continental crust. *Geochim. Cosmochim. Acta* **59**, 1217–1232 (1995).
31. Righter, K., Humayun, M. & Danielson, L. Partitioning of palladium at high pressures and temperatures during core formation. *Nature Geosci.* **1**, 321–323 (2008).

**Supplementary Information** is available in the online version of the paper.

**Acknowledgements** Support from the Region Ile de France (Sesame), CNRS (INSU-Mi-lourd and SEDIT-CNRS) and IPGP (BQR) is acknowledged. We thank M. G. Jackson for a review. We thank D. Calmels and M. Clog for discussion and comments. We also thank P. Richet, M. Chaussidon and P. Agrinier for comments on an early version of the manuscript. This is IPGP contribution number 3415.

**Author Contributions** J.L. performed sulphur isotope measurements. J.L. and M.M. performed sample preparation. P.C. conceived the project. J.L. took the lead in writing the paper, with substantial contributions from P.C. and M.M.

**Author Information** Reprints and permissions information is available at [www.nature.com/reprints](http://www.nature.com/reprints). The authors declare no competing financial interests. Readers are welcome to comment on the online version of the paper. Correspondence and requests for materials should be addressed to J.L. ([labidi@ipgp.fr](mailto:labidi@ipgp.fr)).

## METHODS

**Sample selection and preparation.** Studied samples were chosen according to their degree of glassiness. They were cleaned in 99.9% ethanol to remove any room dust from the samples. Phenocrysts were removed under a binocular microscope or by magnetic separation, when needed. Samples were then crushed to a grain size smaller than 63  $\mu\text{m}$ .

**Electron microprobe measurement.** Sulphur contents of MORB glasses were determined by electron micro-probe (EMP) analyses on polished sections with a Cameca SX100 at the CAMPARIS facility (Pierre et Marie Curie University). The analytical conditions used were 15 kV accelerating voltage, 100 nA sample current, 20  $\mu\text{m}$  beam size, and 60 s counting time for each point. Ten spots were analysed on each polished section, the calculated mean value being taken as the sulphur content of the sample and the standard deviation of each series of measurements being taken as the  $1\sigma$  uncertainty (around 25 p.p.m.).

A natural pyrite was used as a standard. Results were additionally calibrated using two reference samples: sample JDF D2 (high-sulphur-content standard, with 1,400 p.p.m. sulphur) and ED DR11 1–9 (low-sulphur-content standard, with 731 p.p.m. sulphur). These two standards were analysed alternately every 3 or 4 samples. For chlorine contents (see Supplementary Information), the analytical conditions used were 25 kV accelerating voltage, 500 nA sample current, 20  $\mu\text{m}$  beam size, 100 s counting time for each point. A natural scapolite was used as a standard. In addition, results were systematically calibrated using one reference sample: the south Atlantic ridge sample EW9309 41D-1, for which the chlorine amount has been chemically determined at  $55 \pm 12$  p.p.m. (ref. 32). Ten spots were analysed on each polished section. The calculated mean value was taken as the chlorine content of the sample and the standard deviation of each series of measurements is taken as the  $1\sigma$  uncertainty (10 p.p.m.).

**Sulphur extraction for isotope determination.** Sulphur isotope measurement of sulphide inclusions in 300–400 mg of glass separates were performed after chemical extraction, by gas source isotope ratio mass spectrometry at the Stable Isotope

Laboratory at the Institut de Physique du Globe de Paris. Powdered samples were transferred to a Teflon apparatus like that in ref. 7, where they underwent sub-boiling HF–Cr(II) sulphur extraction. Sulphur released in this process as  $\text{H}_2\text{S}$  was trapped as silver sulphide, which was washed, dried and wrapped in clean Al foil. The sulphur-content measurement performed via the EMP value represents the bulk sulphur content of the sample, compared to our chemical extraction protocol, which is strictly specific to reduced sulphur (see details in ref. 7). Chemical extraction yields (that is, the ratio of chemically extracted reduced sulphur to sulphur determined by EMP) averaged  $101 \pm 4\%$  ( $1\sigma$ ,  $n = 23$ ). Such a good match with EMP data supports the absence of significant amounts of oxidized sulphur in these basalts, in agreement with synchrotron spectroscopic results in worldwide samples<sup>18</sup>.

The sulphur isotope measurements were then performed using a dual-inlet MAT 253 gas-source mass spectrometer. Weighed silver sulphide wrapped in aluminium foil was placed into Ni-reaction bombs for fluorination with 250 torr of purified  $\text{F}_2$  at 250 °C overnight. The produced  $\text{SF}_6$  was then purified from impurities in a vacuum line using cryogenic methods and subsequently by gas chromatography separation. Purified  $\text{SF}_6$  was then quantified and analysed in the mass spectrometer, where  $m/z = 127+$ ,  $128+$ ,  $129+$  and  $131+$  ion beams are monitored. The quality of the measurements was estimated on the basis of long-term reproducibility for IAEA reference materials. Repeated analyses gave  $\delta^{34}\text{S} = -0.29 \pm 0.04\%$ ,  $\Delta^{33}\text{S} = +0.082 \pm 0.004\%$ ,  $\Delta^{36}\text{S} = -0.91 \pm 0.11\%$  for IAEA S1 (all errors are  $1\sigma$ ,  $n = 43$ ) and  $\delta^{34}\text{S} = +22.33 \pm 0.06\%$ ,  $\Delta^{33}\text{S} = +0.030 \pm 0.006\%$ ,  $\Delta^{36}\text{S} = -0.17 \pm 0.07\%$  for IAEA S2 (all errors are  $1\sigma$ ,  $n = 20$ ). These values are in agreement with data reported by other laboratories worldwide.

For each MORB glass sample, the sulphur isotope measurement was duplicated and the standard deviation between the two duplicates was taken as the  $1\sigma$  external uncertainty. The standard  $\delta^{34}\text{S}$  uncertainty is 0.01%–0.15%, whereas it is approximately 0.010‰ and 0.100‰ for  $\Delta^{33}\text{S}$  and  $\Delta^{36}\text{S}$ , respectively.

32. Bonifacie, M. *et al.* The chlorine isotope composition of Earth's mantle. *Science* **319**, 1518–1520 (2008).